Studying the Effect of Counter Ions on the Gas Selectivity and Volatile Organic Compounds Separation

Fatimah Edhaim[1] andAlexander Rothenberger[1]
[1]*Physical Science and Engineering Division, King Abdullah University of Science and Technology, Thuwal, Kingdom of Saudi Arabia*

ABSTRACT:*The synthesis and characterization of three new metal chalcogenide aerogels, Chalcogels, $AFe_3Zn_3S_{17}$ (A= Na, K, or Rb) is described. Alkali metal polychalcogenides (Na_2S_5, K_2S_5, or Rb_2S_5) reactwith metal acetate like $Fe(OAc)_2$ and $Zn(OAc)_2$in formamide solutionforming extended polymeric frameworks by gelation. Chalcogels obtained aftersupercritical drying have BET surface areas of 430, 444, and 435 m^2/g for $NaFe_3Zn_3S_{17}$, $KFe_3Zn_3S_{17}$, and $RbFe_3Zn_3S_{17}$, respectively. The effect of the counter ions (K, Na, and Rb) wasstudied by examined the adsorption capacities of the resulting chalcogels toward different gases and volatile organic compounds. The measurements showed that CO_2 and toluene adsorption capacities increase with the polarizability of the surface atoms in the following order: Rb chalcogel> K chalcogel> Na chalcogel.This finding reveals a trend based on cation size and acid–base surface properties that might have a significant impact on altering adsorptive properties of chalcogels by using more polarizable counter ions.*

KEYWORDS –*Adsorption, Chalcogel, Gas and hydrocarbon selectivity, Mesoporous, Separation*

I. INTRODUCTION

Volatile organic compounds (VOCs) term represent a broad range of chemical substances that are frequently used and emitted from chemical and petrochemical industries. These materials are considered to be one of the major air pollutants as they contribute to the depletion of the ozone layer, and increase the global warming. Moreover, some of them are harmful to humans, plants, and animals. Owing to their volatile nature, they rapidly combine with the atmospheric air forming fog. Therefore, it is important to innovate systems to reduce the emission of VOCs into the atmosphere in an efficient and economical manner.

Several techniques have been developed to lessen the emission of such toxic materials such as filtration, distillation, and absorption separation. Of these technologies, adsorption-using membranes like zeolite, polymeric resins, and silica gel has been known as an effective, relatively inexpensive and high selective method for the efficient removal of VOCs.[1]

Recently, metal chalcogenide aerogels or chalcogels have been described as adsorbents for selective separations of VOCs.[2]Chalcogels are amorphous porous materials in which chalcogenide building blocks are connected to transition metal ions forming polymeric frameworks.[3]Unlike most porous materials, which have surfaces covered with carbon or oxygen,[3] Chalcogels have surfaces coated with more polarizable and softer chalcogen ions, $[Q_x]^{2-}$ (Q= S, Se, and Te; x= 1-5),[3-4] which provide an opportunity to explore interactions with different molecules.

Chalcogels are usually synthesized using thesol-gel metathesis route, which allows the usage of various molecular chalcogenide units to form a wide range of novel porous materials.

Recently, ithas been demonstrated that the metathesis reaction between mixture salts and K_2S_5 in formamide gives rise to amorphous and high surface area chalcogels. These chalcogels have negatively charged networks, which are balanced by K^+ cations.[5] Therefore, these cations are part of the chalcogels and located within the pores to balance the framework charge.

Incorporation of these cations within the chalcogels causes high electrical field gradients inside the pores. Also, the presence of soft and heavy chalcogen atoms like sulfur on the chalcogel surfaces results in basicity of the chalcogel frameworks. Thus, these chalcogels show high selectivity and large adsorption capacities toward acidic gas like CO_2 and volatile hydrocarbon vapor like toluene.

It is well known that polar or polarizable molecules prefer to interact with the cation sites (alkali metal species) within porous materials and get adsorbed on their surfaces. However, the preferential adsorptions of the molecules vary based on the cation types, which induce an electric field inside the pores.

Accessible pore volume and pore size also significantly affect the adsorptive properties of porous materials.

Barthomeuf[6] noticed that the adsorption capacity of faujasites containing larger alkali metals, as charge compensating, toward payroll (acid probe molecules) is greater than those with a smaller cation size. The low electronegativity of large alkali metal ions enhances the negative charge on the pore frameworks, and hence, increases the basicity of the porous materials. Therefore, it is reasonable to expect porous adsorbents containing large cations like Cs, Rb or K could have higher adsorption capacities for acidic adsorbates than those with smaller size such as Li or Na.

Talu and coworkers[7] studied the influence of ion exchange of alkaline earth metals in Y and Z zeolites on the methane adsorption. He observed improvement of zeolite capacity toward methane with increasing cation size. Talu proposed that the small alkaline earth cations were shielded by some cavities' molecules and limited from the interactions with adsorbates. The shielding effect, however, does not exist with the large cations, and hence more adsorbate molecules would be affected and got adsorbed.

The effect of counter-ions on the adsorption properties has frequently been studied in zeolites. However, up to date, there are no studies reported about the counter-ion effects onto metal chalcogels. Therefore, we have been motivated to investigate the influence of different alkali metals on the adsorption capacity of chalcogels. Chalcogels containing K^+ have been investigated for gas and volatile hydrocarbon separation, but the effect of the presence of different alkali metals (K, Na, or Rb) on the adsorption properties of chalcogels has not been studied and hence is worth to be further investigated.

In this work, we synthesized three amorphous and high surface area chalcogels $AFe_3Zn_3S_{17}$ (A= Na, K, or Rb) and examined the effect of present different counter-ion size on the VOCs separation and selective gas adsorption. The higher adsorption capacity of CO_2 and toluene vapor was found in the following order: $RbFe_3Zn_3S_{17}$> $KFe_3Zn_3S_{17}$> $NaFe_3Zn_3S_{17}$. Our measurements revealed that the adsorption capacity of Rb forms, where the polarizability (cation size) and acid–base surface properties are dominant, is the greatest.

II. EXPERIMENTAL

2.1 Synthesis

Zinc acetate (Alfa, anhydrous 99.98%), Iron(II) acetate (Strem Chemicals, 97% anhydrous), formamide (acros, 99.5%), absolute ethanol (Aldrich, 99.8%), toluene (Fisher Scientific, 99.9%) and cyclohexane (Roth Chemicals, 99.5%) were used as received. Na_2S_5, K_2S_5, and Rb_2S_5 were freshly prepared according to the literature procedure(Fig.S1, Supporting Information)[8]The solvents were degased for around 12 h by bubbling N_2 gas, then placed inside a nitrogen-filled glovebox ($c(O_2)$ < 0.1 ppm, $c(H_2O)$ < 0.1 ppm). Synthesis of the chalcogels and solvent exchange were achieved inside a glovebox under nitrogen.

2.2 Synthesis of $NaFe_3Zn_3S_{17}$, $KFe_3Zn_3S_{17}$and $RbFe_3Zn_3S_{17}$ Chalcogels

An amount of 17.39mg (0.1mmol) $Fe(OAc)_2$and 18.34mg (0.1mmol) $Zn(OAc)_2$were dissolved in 1.5 ml of formamide and mixed with another 1.5 ml of formamide solution containing 41.26 mg, 47.70mg or 66.25mg (0.2 mmol) of Na_2S_5, K_2S_5or Rb_2S_5, respectively. Upon mixing the two solutions, a clear dark black solution was obtained. The viscosity of these solutions significantly increased, and the solutions solidified into black monolithic wet gels in a minimum one-week. The residual formamide was poured, and the wet gels were subsequently washed with absolute ethanol from 8 to 10 times to remove all unreacted precursors and counter ions. The wet gels then were dried using supercritical drying with CO_2 at 35^{o}C to obtain superfine black chalcogels.

III. RESULTS AND DISCUSSION

In this study, polychalcogenide clusters (Na_2S_5, K_2S_5,or Rb_2S_5) and metal ion linkers (Fe^{2+} and Zn^{2+}) were separately dissolved in formamide and mixed at room temperature. During aging period, the mixtures were left undisturbed for a week to allow the viscosity of the solution to increase gradually and form a rigid gel, Fig.1; the color also became darker indicating gradual polymerization. The resulting wet gels then undergo solvent exchange followed by supercritical CO_2 drying processes to produce aerogels. The final metal chalcogenide aerogels are brittle with black and very lightweight particles.

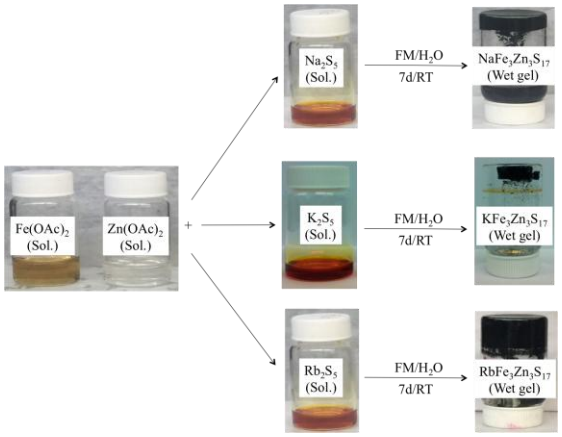

Figure1 Visual representation of the sol–gel process in formamide solutions (FM) at room temperature (RT), before the solvent exchange, showing the completed metathesis reaction of wet gels.

3.1 Characterization

The porous morphology, spongy nature and smooth surface structures of the chalcogels have been detected by the scanning electron microscopy (SEM) technique. The absence of dark areas in micro scale demonstrated single-phase chalcogels. The aggregation of the primary particles of nanometer size forms the secondary (large) particles of micrometer size (Fig. 2 A (a) B (a) and C (a)).

Transmission electron microscope (TEM) results confirm the random porosities within the framework (Fig. 2 A (b), B (b) and C (b)). Electron diffraction studies of multiple regions of the samples prove the absence of any crystalline phases, inset of Fig. 2 (A, B, C).

Energy dispersive spectroscopy analysis (EDS) approve that not only transition metals and the polysulfide species are present, but alkali metals (Na, K, Rb) also incorporate as a part of the chalcogels. The average percentage of each element is summarized in Fig. S2, Supporting Information.

FTIR analyses have been recorded to reveal any residual species of organic materials after drying processes. Some vibration bands that are assigned to the residual amount of formamide species have been observed; indicating a trace amount of formamide is incorporating within the chalcogel frameworks (Fig. S3, Supporting Information).

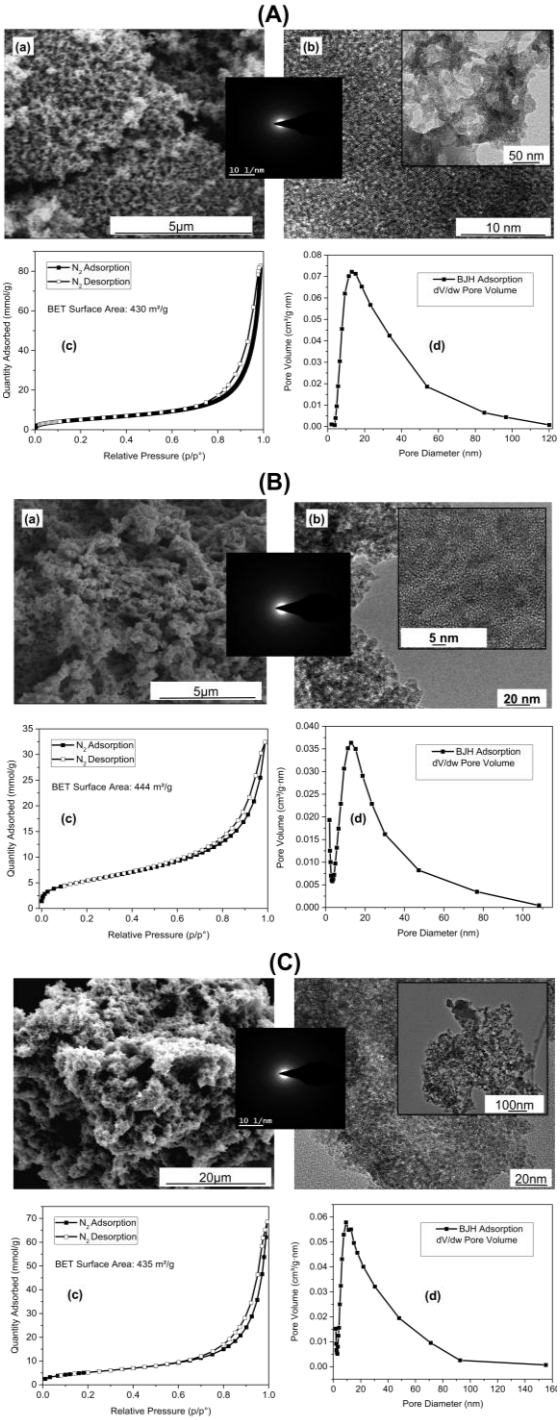

Figure 2 Characterization and properties of the (A) $NaFe_3Zn_3S_{17}$, (B) $KFe_3Zn_3S_{17}$, and (C) $RbFe_3Zn_3S_{17}$gels. (a) Scanning electron microscope (SEM) showing fluffy features throughout the micron sized specimens and porous nature of these materials. (b) Low and high magnification transition electron microscope (TEM) images showing a nano-scale porous structure of chalcogel. Multiple diffraction rings (inset) confirms the absence of crystalline structure within the chalcogel network. (c) Nitrogen adsorption–desorption isotherm. (d) Pore-size distribution plot calculated from the adsorption isotherm by the BJH method.

Thermogravimetric (TGA) results of the super-critically dried chalcogel materials show small weight loss up to 150°C (4, 7 and 3 %) for $NaFe_3Zn_3S_{17}$, $KFe_3Zn_3S_{17}$and $RbFe_3Zn_3S_{17}$, respectively, which can be attributed to evaporation of chemisorbed or physisorbed solvent (Fig. S4, Supporting Information). The weight loss from 200°C to 400°C attributed to the loss of sulfur from the inorganic frameworks, as approved by EDS after TGA(Fig. S5, Supporting Information). The total weight loss up to 600°C is 45%, 85% and 40% for $NaFe_3Zn_3S_{17}$, $KFe_3Zn_3S_{17}$,and $RbFe_3Zn_3S_{17}$, respectively.

The powder XRD patterns for the tested chalcogels indicated in the Fig. S6, Supporting Information. Recorded patterns support the electron diffraction data and confirm the absence of any crystalline phase.

3.2 Adsorption Studies

Nitrogen physisorption isotherms of the resulting samples at 77 K, total pore volume and BET (Brunauer Emmett Teller) surface area were determined using ASAP 2020, Micromeritics Instruments. The resulting chalcogels possess similar adsorption isotherms to the reported chalcogels[9](Fig.2 A (c), B(c) and C (c)). The contribution of micropores (d < 2 nm) indicated by the minor adsorption at very low pressures (P/Po < 0.05). The most adsorption occurred at high pressures (0.7 < P/Po < 1.0) where the macropores (d > 50 nm) and mesopores (2 < d < 50 nm) are the most contribute. The small hysteresis loop demonstrated the slower desorption rate of nitrogen comparing to the adsorption rate due to the percolation effect of variable pore size.

The high BET surface areas (430, 444 and 435 m^2/g) of $NaFe_3Zn_3S_{17}$, $KFe_3Zn_3S_{17}$and $RbFe_3Zn_3S_{17}$ chalcogels, respectively, confirm the pore structures of the chalcogels. The broad pore size distribution of the chalcogels was established from BJH pore size isotherms (Fig.2 A (d), B(d) and C (d)). The average pore diameter of the resulting materials ranges from 24nm ($NaFe_3Zn_3S_{17}$)to 20 nm ($KFe_3Zn_3S_{17}$ and $RbFe_3Zn_3S_{17}$), as calculated from the total pore volume and surface area with a rough approximation of the pore shape as cylindrical and slit.

The skeletal density of the chalcogels was 2.37 g cm^{-3} for $NaFe_3Zn_3S_{17}$, 2.39 g cm^{-3} for $KFe_3Zn_3S_{17}$ and 2.43 g cm^{-3} for $RbFe_3Zn_3S_{17}$ chalcogel.

To evaluate the effect of alkali metals on the adsorption properties of the chalcogels, we tested the adsorption capacity of the targeted calcogels with various volatile hydrocarbons (*e.g.,* toluene and cyclohexane) at room temperature. Based on the recorded isotherms(Fig.3), the toluene uptake of both chalcogels is much higher than cyclohexane uptake, which suggests a strong interaction between chalcogel surface and polarizable molecules of toluene (polarity index is 2.4). Enhancement of the adsorption capacity of toluene is also possible through π-complexation interaction.[10]

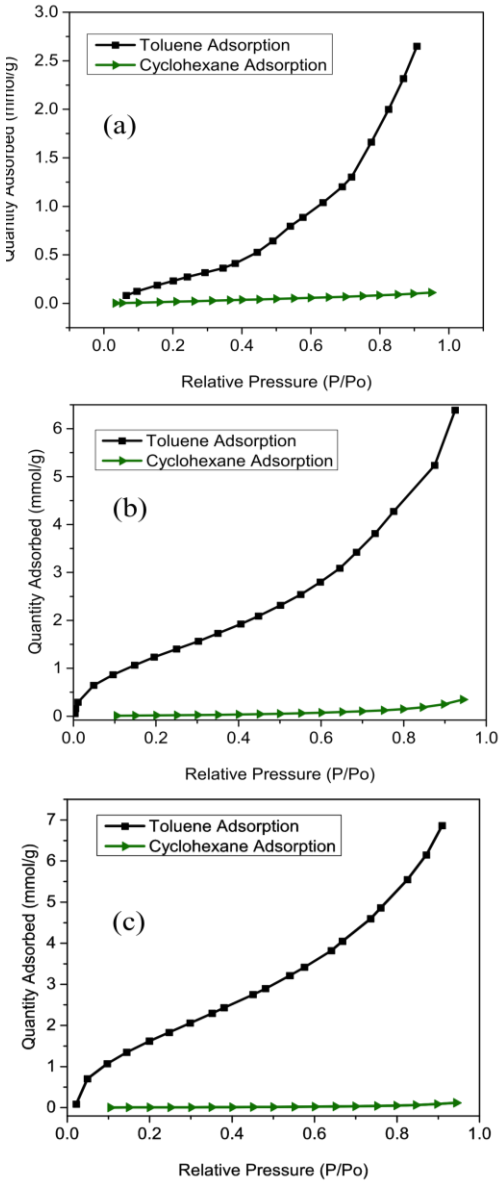

Figure 3 Adsorption isotherms of toluene and cyclohexane at room temperature in (a) $NaFe_3Zn_3S_{17}$, (b) $KFe_3Zn_3S_{17}$, and (c) $RbFe_3Zn_3S_{17}$ chalcogels

The quantity adsorbed of toluene on the $NaFe_3Zn_3S_{17}$, $KFe_3Zn_3S_{17}$and $RbFe_3Zn_3S_{17}$ chalcogels is 2.7, 6.4, and 7.3 mmol/g, respectively, as indicated in the toluene isotherms(Fig.3). These results indicate that chalcogels containing larger

cations have higher capacities for hydrocarbon vapor. The presence of large cations within the chalcogels induces larger electrical field than the small cations, leading to higher adsorption capacity. Also, it has been reported that small cations can create week π–cation interactions,[11] and hence lower toluene vapor adsorption occurred on $NaFe_3Zn_3S_{17}$ than $KFe_3Zn_3S_{17}$ and $RbFe_3Zn_3S_{17}$ chalcogels, Table 1.

Table 1 Comparison of toluene adsorption capacity at 298 K.

Adsorbent	Surface Area (m^2/g)	Toluene adsorption (mmol/g)
$NaFe_3Zn_3S_{17}$	430	2.7
$KFe_3Zn_3S_{17}$	444	6.4
$RbFe_3Zn_3S_{17}$	435	7.3

The chalcogels were also investigated for CO_2, CH_4 and H_2 separation at different temperatures. The isotherms reveal that the adsorption capacity of the chalcogels increased with increasing the cation size. All of the chalcogels demonstrated higher adsorption of CO_2 than CH_4 and H_2 over the chalcogels (Fig. 4, and Fig. S7, Supporting Information). These results can be explained by polarization. As CO_2 is more polarizable than CH_4 and H_2, more interactions with the polarizable surface of the chalcogels through dispersion force could occur (polarizability α in units of 10^{-24} cm^3: α (CO_2) = 2.9 > α (CH_4) = 2.6 > α (H_2) = 0.8).[4] We also observed that the adsorption capacity of the chalcogels toward CO_2 increased in the following order: $RbFe_3Zn_3S_{17}$> $KFe_3Zn_3S_{17}$ > $NaFe_3Zn_3S_{17}$. The adsorption capacity of the chalcogels and the strength of the adsorption can be controlled by the interactions between the electric field, produced by the cations on the adsorbent surfaces, and the adsorbate molecules. As the Rb ions are larger and more polarizable than the Na or K ions, more electrostatic interactions can be induced on the $RbFe_3Zn_3S_{17}$, and hence more adsorption occurred. The acid–base features of the chalcogel frameworks also contributed in improving adsorption properties. The cations are acid species, and the sulfidic surfaces next to the cations act as basic sites. As the cation size increases, the basicity sulfidic surfaces increases because the lower electronegativity of the alkali metal cations induced the negative charge on the sulfur atoms in the frameworks. Thus, it is logical to expect chalcogels with larger cations like Rb would have more adsorption capacity for acidic adsorbates like CO_2.

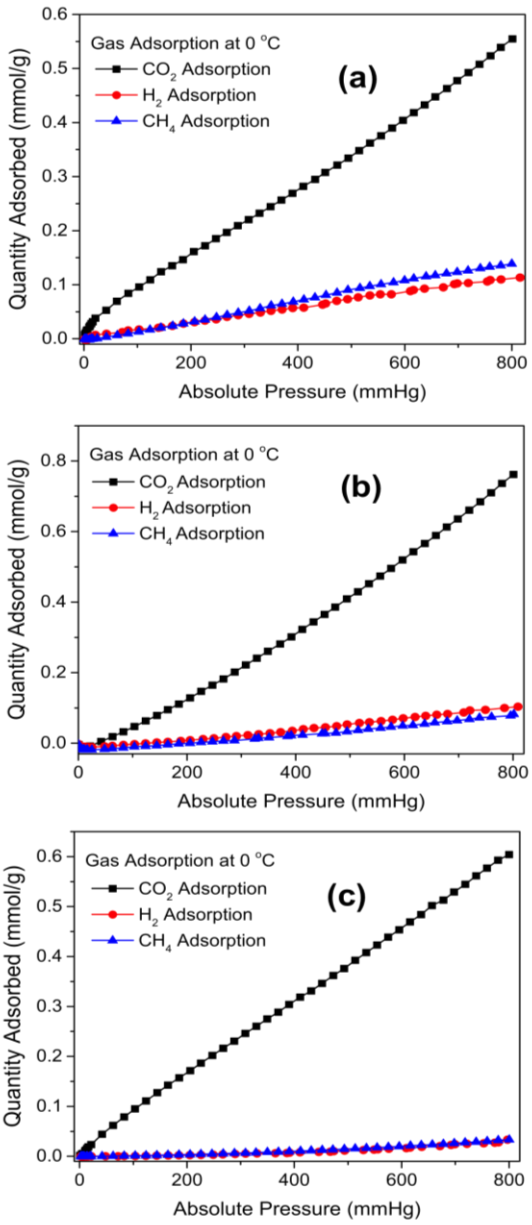

Figure 4 Gas adsorption isotherms of CO2, CH4, and H2 observed (a) $NaFe_3Zn_3S_{17}$, (b) $KFe_3Zn_3S_{17}$, and (c) $RbFe_3Zn_3S_{17}$ at 0 °C.

The presence of large rubidium atoms renders pore surface of the sulfidic chalcogels more polarizable, and this is reflected in its selectivity toward gases. Prediction of gas selectivity using the ideal adsorbed solution theory (IAST) from single component isotherms showed almost double selectivity values (CO_2/H_2: 180 and CO_2/CH_4: 60) for $RbFe_3Zn_3S_{17}$ compared to $KFe_3Zn_3S_{17}$ chalcogels with selectivity values (CO_2/H_2: 120 and CO_2/CH_4: 35). $RbFe_3Zn_3S_{17}$ also reveal around four times higher selectivity than $NaFe_3Zn_3S_{17}$ chalcogel (CO_2/H_2: 11 and CO_2/CH_4: 5) (Fig. 5, Table 2). This again revealed the reactivity of acidic CO_2 toward the

basic characteristic of the chalcogels containing large cations. This finding indicates that adsorption property of the chalcogel depends on the chemical composition of the chalcogels and the cations present within the pore frameworks.

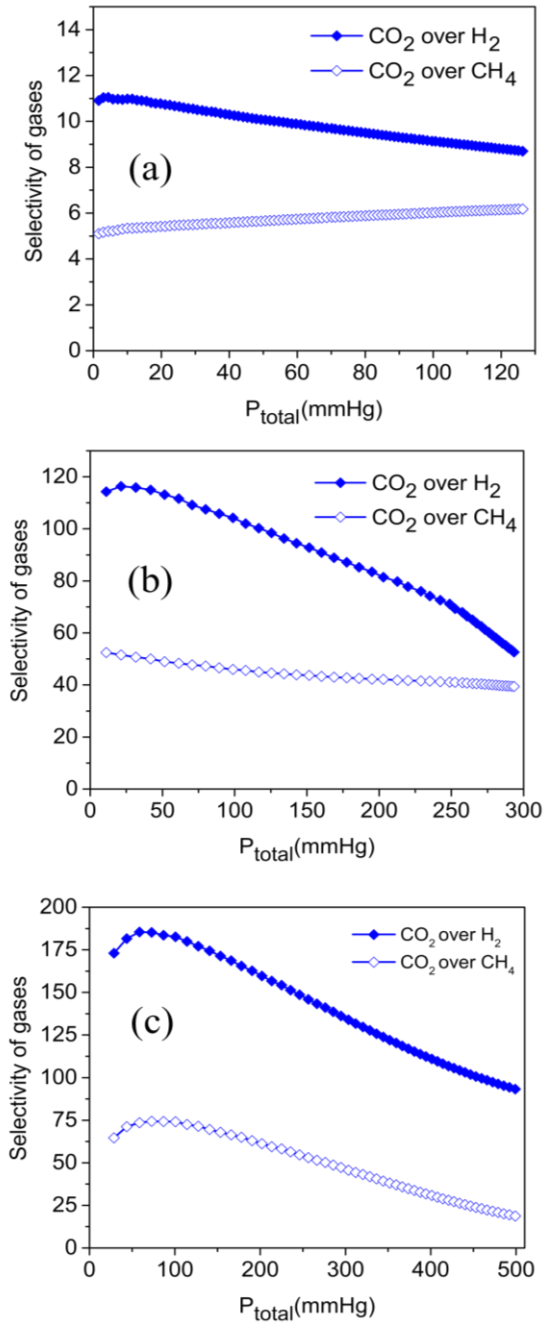

Figure 5 Selectivity of CO_2 over H_2 and CO_2 over CH_4in (a) $NaFe_3Zn_3S_{17}$, (b) $KFe_3Zn_3S_{17}$, and (c) $RbFe_3Zn_3S_{17}$as predicted by IAST for equimolar mixtures of CO_2/H_2 and CO_2/CH_4 at 273 K (Ptotal is the total pressure of the gas mixture).

Table 2 Ionic radii of alkali metals and Selectivity of the corresponding calcogels

Cation	Radius (A˚)	Corresponding Chalcogel	Selectivity CO_2/CH_4, CO_2/CH_4
Na^+	0.97	$NaFe_3Zn_3S_{17}$	11, 5
K^+	1.33	$KFe_3Zn_3S_{17}$	120, 35
Rb^+	1.47	$RbFe_3Zn_3S_{17}$	180, 74

IV. CONCLUSIONS

Three chalcogels ($NaFe_3Zn_3S_{17}$, $KFe_3Zn_3S_{17}$and $RbFe_3Zn_3S_{17}$) have been synthesized using the sol-gel metathesis reaction. The resulting chalcogels possess high BET surface areas and are capable of separation of different hydrocarbons and gases. The results demonstrated that the largest capacities toward toluene and CO_2 vapor were achieved by chacogels containing the large Rb cations because they have larger polarizability, and can induce more electrostatic interaction than smaller cations. These results indicate that adsorption properties of the chalcogels could be improved by altering the composition of the materials.

V. Acknowledgements

This work was supported by King Abdullah University of Science and Technology, KAUST. We thank Dr. Rachid Sougrat(Advanced Nanofabrication, Imaging, and Characterization Core Lab) for TEM analysis.

REFERENCES

[1] a) D. Romero, D. Chlala, M. Labaki, S. Royer, J.-P. Bellat, I. Bezverkhyy, J.-M. Giraudon, J.-F. Lamonier, Removal of Toluene over NaX Zeolite Exchanged with Cu2+, *Catalysts, 3(5)*, 2015, 1479-1497; b) S. Calero, P. Gomez-Alvarez, On the performance of FAU and MFI zeolites for the adsorptive removal of a series of volatile organic compounds from air using molecular simulation, *PCCP, 17(39)*, 2015, 26451-26455; c) Y. Yu, L. Zheng, J. Wang, Adsorption Behavior of Toluene on Modified 1X Molecular Sieves, *J. Air Waste Manage. Assoc., 62(10)*, 2012, 1227-1232; d) K. Wormeyer, I. Smirnova, Adsorption of CO2, moisture and ethanol at low partial pressure using aminofunctionalised silica aerogels, *Chem. Eng. J., 225(*2013, 350-357; e) H. Wang, M. Tang, K. Zhang, D. Cai, W. Huang, R. Chen, C. Yu, Functionalized hollow siliceous spheres for VOCs removal with high efficiency and stability, *J. Hazard. Mater., 268(*2014, 115-123; f) C. Long, W. Yu, A. Li, Adsorption of n-hexane vapor by macroporous and hypercrosslinked polymeric resins: Equilibrium and breakthrough analysis, *Chem. Eng. J., 221(*2013, 105-110; g) E. J. Simpson, R. K. Abukhadra, W. J. Koros, R. S. Schechter, Sorption equilibrium isotherms for volatile organics in aqueous solution. Comparison of head-space gas chromatography and on-line UV stirred cell results, *Ind. Eng. Chem. Res., 32(10)*, 1993, 2269-2276.

[2] a) F. Edhaim, A. Rothenberger, Rare Earth Chalcogels NaLnSnS4 (Ln = Y, Gd, Tb) for Selective Adsorption of Volatile Hydrocarbons and Gases, *Z. Anorg. Allg. Chem.*, 2017; b) E. Ahmed, J. Khanderi, D. H. Anjum, A. Rothenberger, Selective Adsorption of Volatile Hydrocarbons and Gases in High Surface Area

Chalcogels Containing [ES3]3– Anions (E = As, Sb), *Chem. Mater.*, *26(22)*, 2014, 6454-6460.

[3] Y. Oh, S. Bag, C. D. Malliakas, M. G. Kanatzidis, Selective Surfaces: High-Surface-Area Zinc Tin Sulfide Chalcogels, *Chem. Mater.*, *23(9)*, 2011, 2447-2456.

[4] M. Shafaei-Fallah, A. Rothenberger, A. P. Katsoulidis, J. He, C. D. Malliakas, M. G. Kanatzidis, Extraordinary Selectivity of CoMo3S13 Chalcogel for C2H6 and CO2 Adsorption, *Adv. Mater.*, *23(42)*, 2011, 4857-4860.

[5] M. Shafaei-Fallah, J. Q. He, A. Rothenberger, M. G. Kanatzidis, Ion-Exchangeable Cobalt Polysulfide Chalcogel, *JACS*, *133(5)*, 2011, 1200-1202.

[6] D. Barthomeuf, Conjugate acid-base pairs in zeolites, *J. Phys. Chem.*, *88(1)*, 1984, 42-45.

[7] a) S. Y. Zhang, O. Talu, D. T. Hayhurst, High-pressure adsorption of methane in zeolites NaX, MgX, CaX, SrX and BaX, *J. Phys. Chem.*, *95(4)*, 1991, 1722-1726; b) O. Talu, S. Y. Zhang, D. T. Hayhurst, Effect of cations on methane adsorption by NaY, MgY, CaY, SrY, and BaY zeolites, *J. Phys. Chem.*, *97(49)*, 1993, 12894-12898.

[8] Y. Oh, C. D. Morris, M. G. Kanatzidis, Polysulfide Chalcogels with Ion-Exchange Properties and Highly Efficient Mercury Vapor Sorption, *JACS*, *134(35)*, 2012, 14604-14608.

[9] a) S. Bag, A. F. Gaudette, M. E. Bussell, M. G. Kanatzidis, Spongy chalcogels of non-platinum metals act as effective hydrodesulfurization catalysts, *Nature. Chem.*, *1(3)*, 2009, 217-224; b) S. Bag, P. N. Trikalitis, P. J. Chupas, G. S. Armatas, M. G. Kanatzidis, Porous Semiconducting Gels and Aerogels from Chalcogenide Clusters, *Science*, *317(5837)*, 2007, 490.

[10] X. Lin, A. J. Blake, C. Wilson, X. Z. Sun, N. R. Champness, M. W. George, P. Hubberstey, R. Mokaya, M. Schröder, A Porous Framework Polymer Based on a Zinc(II) 4,4‘-Bipyridine-2,6,2‘,6‘-tetracarboxylate: Synthesis, Structure, and “Zeolite-Like” Behaviors, *JACS*, *128(33)*, 2006, 10745-10753.

[11] D. A. Dougherty, The Cation−π Interaction, *Acc. Chem. Res.*, *46(4)*, 2013, 885-893.

Supplementary Figures:

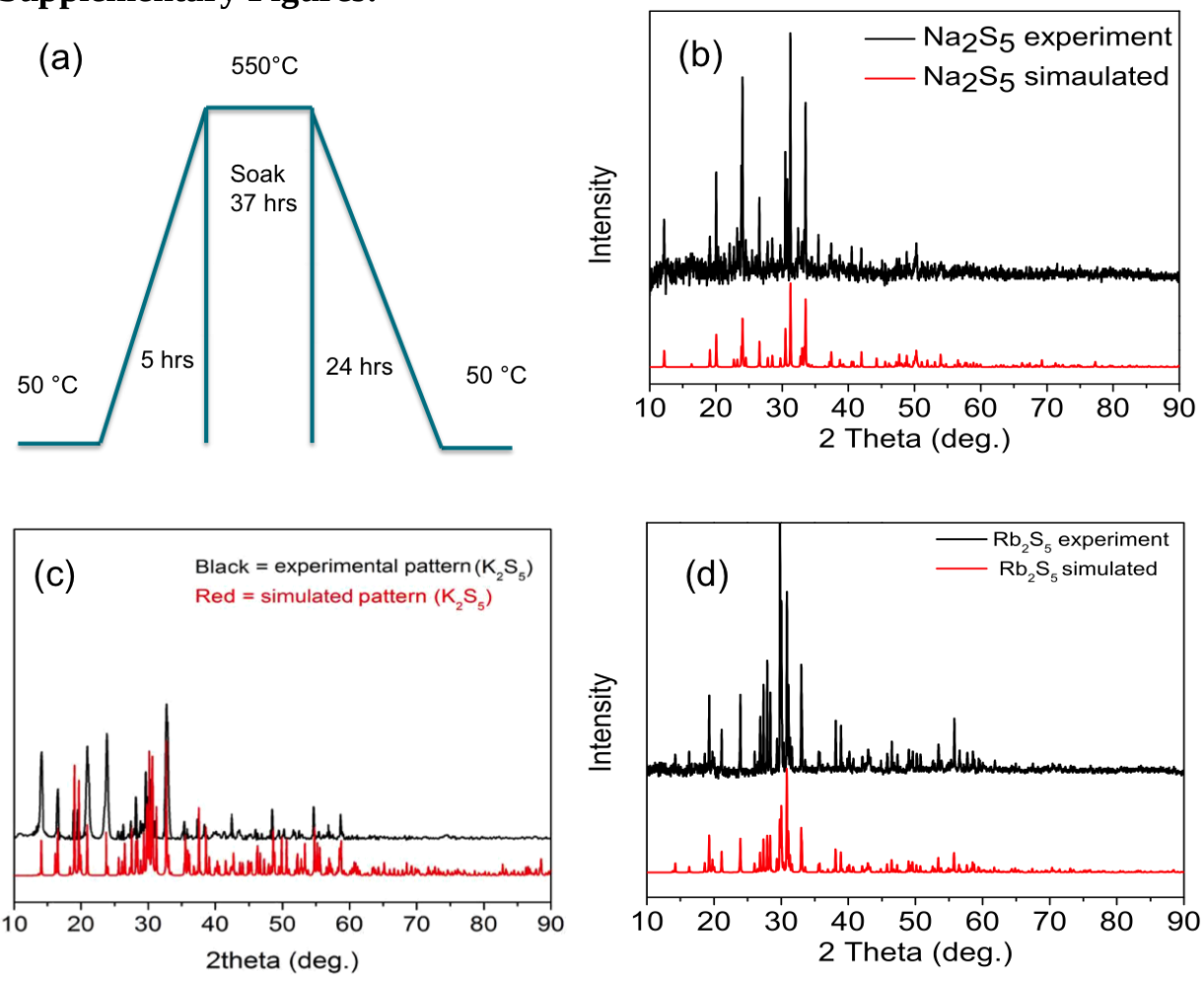

Figure S1a) Experimental procedure of starting material A_2S_5 (A= Na, K, and Rb), (b, c and d) Powder XRD patterns of the starting materials A_2S_5 (A= Na, K, and Rb), respectively, confirming their purity.

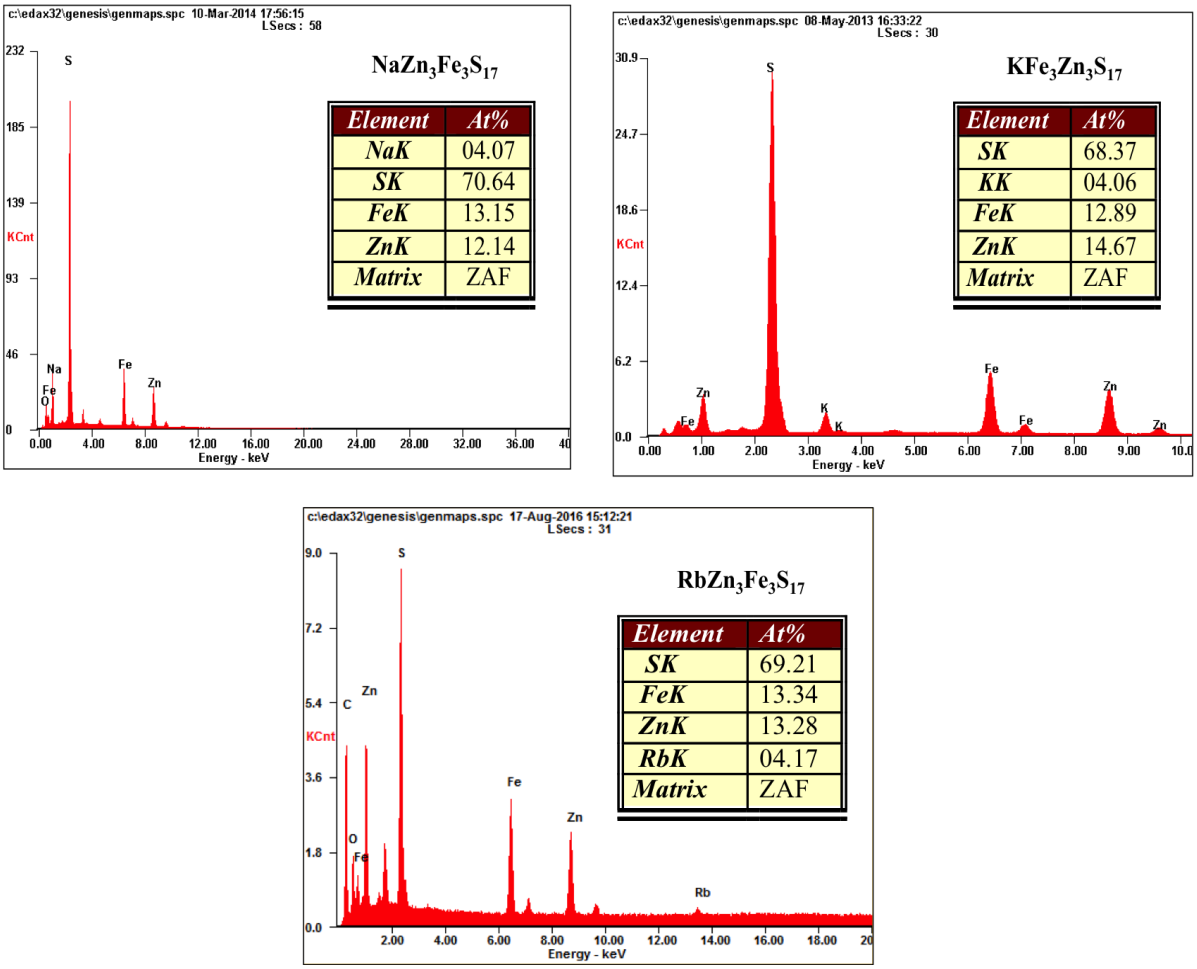

Figure S2EDS result of the resultingchalcogels after drying. Inset the table of the elements showing the average composition.

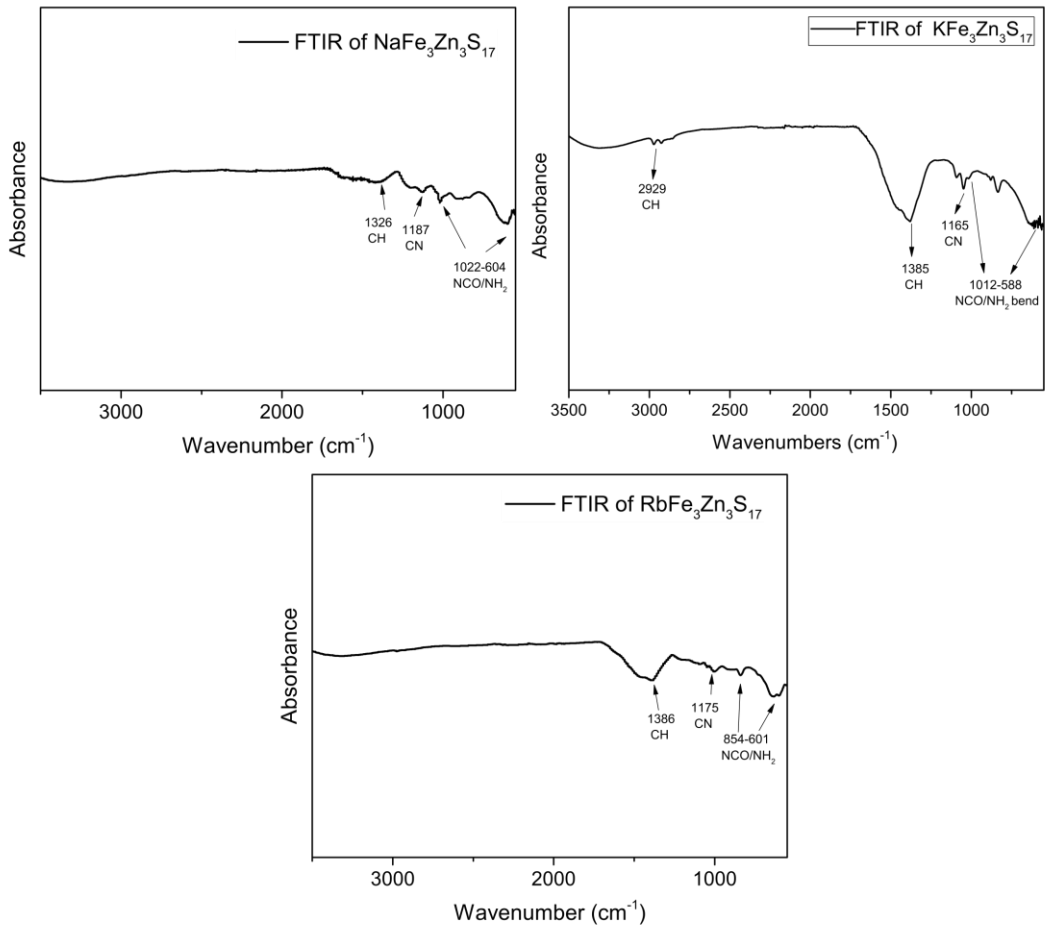

Figure S3 FTIR spectra showing some vibration peaks belong to the formamide species.

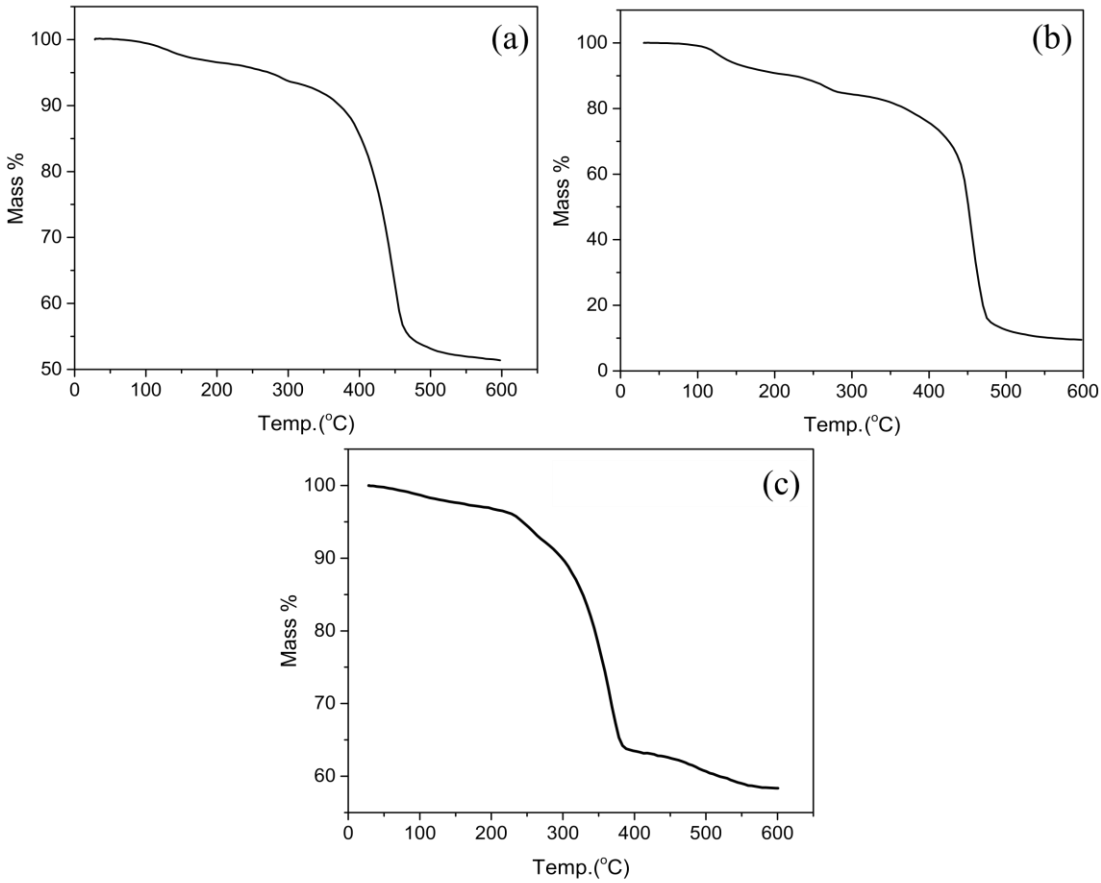

Figure S4TGA of the resulting chalcogels showing gradual weight loss of (a) $NaFe_3Zn_3S_{17}$, (b) $KFe_3Zn_3S_{17}$ and (c) $RbFe_3Zn_3S_{17}$ chalcogels, under 20 ml min^{-1} of nitrogen flow and 10 K min^{-1} of heating rate.

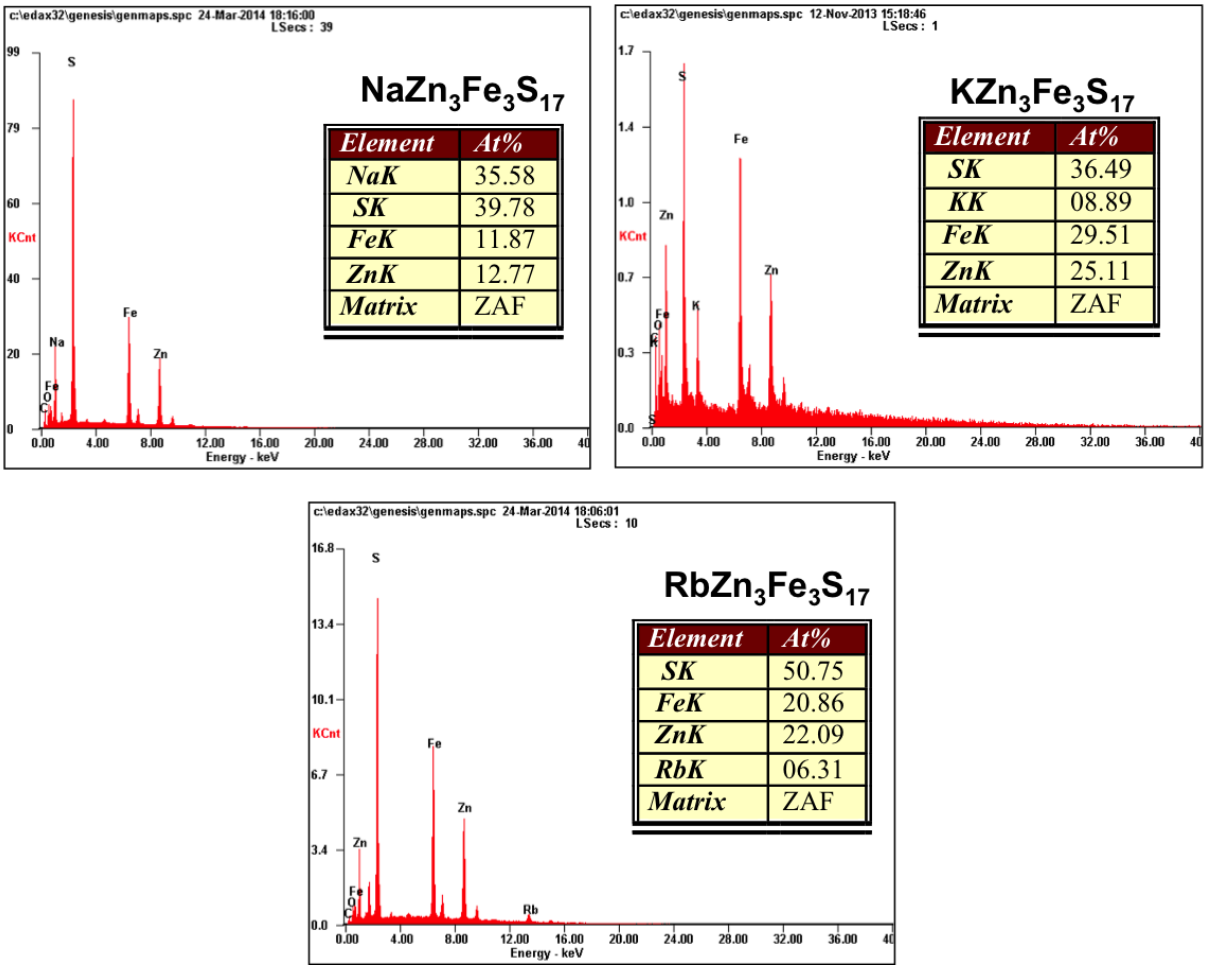

Figure S5EDS analysis after TGA of the resulting chalcogelsshowing the residual of the chalcogel.

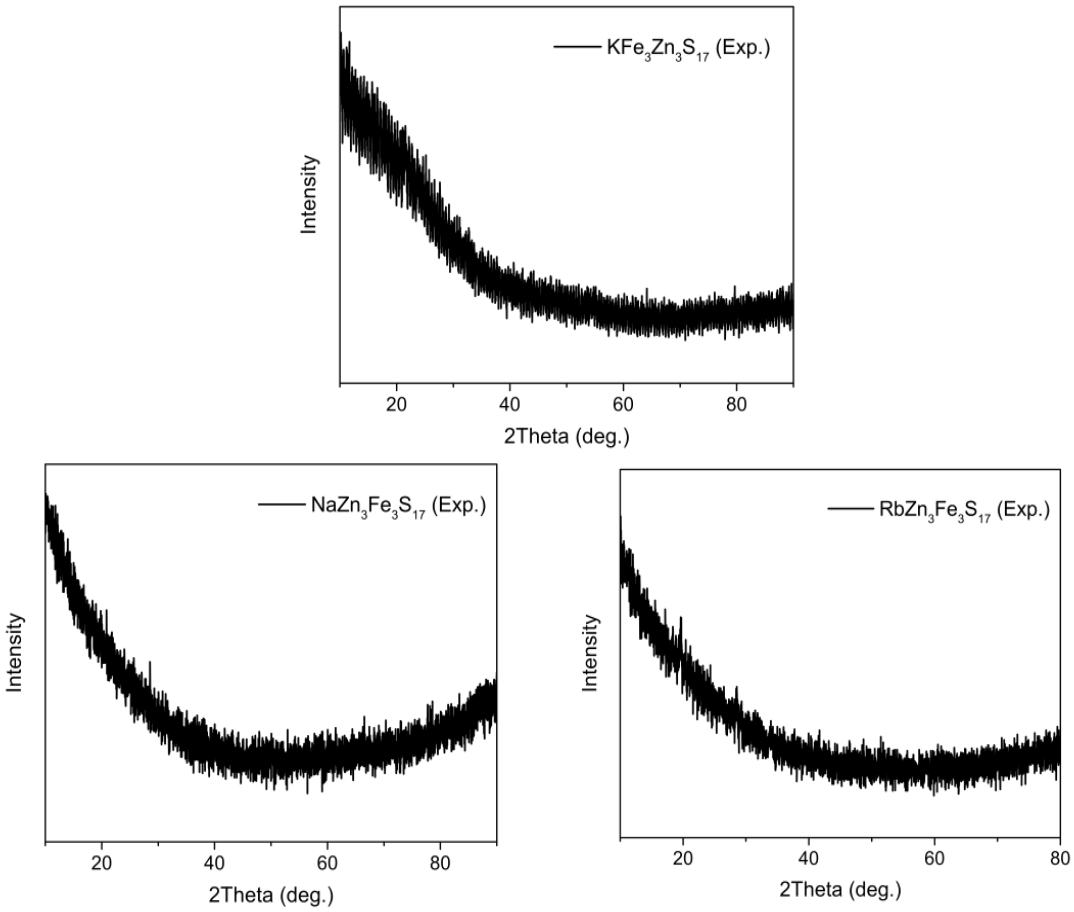

Figure S6 Powder XRD resultsshow the amorphous nature of the prepared chalcogenide aerogels.

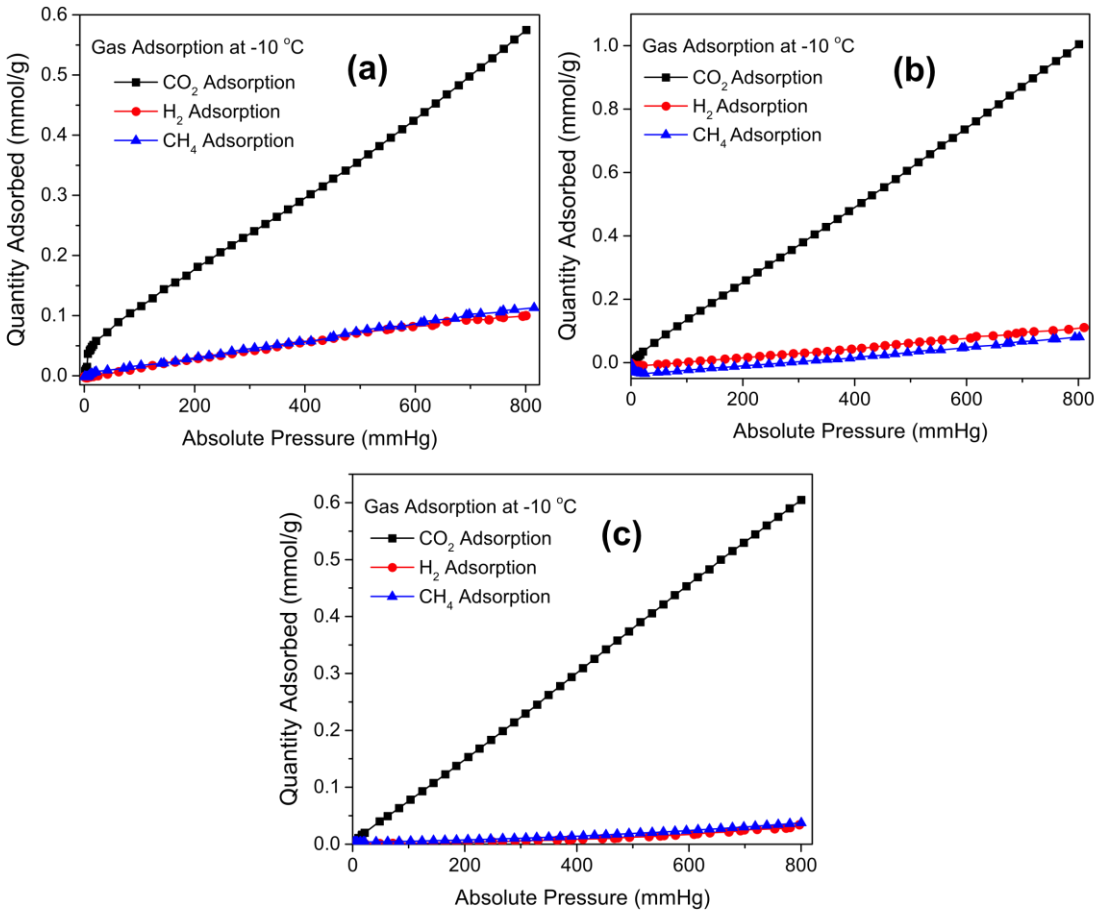

Figure S7 Gas adsorption isotherms of CO_2, CH_4, and H_2 observed (a) $NaFe_3Zn_3S_{17}$, (b) $KFe_3Zn_3S_{17}$ and (c) $RbFe_3Zn_3S_{17}$ at -10 °C.